Письма в ЭЧАЯ. 2008. Т. 5, № 2(144). С. 202–218

ELECTRON/PION IDENTIFICATION IN THE CBM TRD APPLYING A ω_n^k GOODNESS-OF-FIT CRITERION

E. P. Akishina [a], *T. P. Akishina* [a], *V. V. Ivanov* [a], *A. I. Maevskaya* [b], *O. Yu. Denisova* [a]

[a] Joint Institute for Nuclear Research, Dubna
[b] Institute for Nuclear Research, Troitsk, Russia

The problem of electron/pion identification in the CBM experiment based on the measurements of energy losses and transition radiation in the TRD detector is discussed. Earlier we analyzed a possibility to solve such a problem using an artificial neural network (ANN) [1]. Here we consider an approach based on a nonparametric ω_n^k goodness-of-fit criterion, comparison with the ANN method is also performed. We show that both methods provide a comparable level of pion suppression and electron identification, the ω_n^k test is more simple for practical applications, the ANN method provides the needed level of pions suppression only if «clever» variables are used. We demonstrate that application of the ω_n^k-criterion to the J/ψ reconstruction provides a high level of pion background suppression and significantly improves a signal-to-background ratio.

Рассмотрена задача идентификации электронов/пионов в эксперименте CBM на основе ионизационных потерь энергии и переходного излучения в детекторе TRD. Ранее [1] была изучена возможность решения этой задачи с помощью искусственной нейронной сети (ИНН). Здесь исследуется возможность решения указанной задачи с помощью непараметрического критерия согласия ω_n^k и проводится его сравнение с методом на основе ИНН. Показано, что оба подхода обеспечивают сопоставимый уровень подавления пионов и идентификации электронов; при этом критерий ω_n^k прост в применении, а ИНН обеспечивает необходимый уровень подавления пионов только при использовании «умных» переменных. Показано, что применение критерия ω_n^k в задаче реконструкции J/ψ-событий обеспечивает высокий уровень подавления фона от пионов и существенно улучшает отношение сигнал/фон.

PACS: 29.40.Cs

INTRODUCTION

The CBM Collaboration [3, 4] builds a dedicated heavy-ion experiment to investigate the properties of highly compressed baryonic matter as it is produced in nucleus–nucleus collisions at the Facility for Antiproton and Ion Research (FAIR) in Darmstadt, Germany. A scientific goal of the research program of the CBM experiment is to explore a phase diagram of strongly interacting matter in the region of the highest baryon densities. This approach is complementary to the activities at RHIC (Brookhaven) and ALICE (CERN–LHC) which concentrate in the region of high temperatures and/or very high baryon densities.

The experimental set-up has to fulfil the following requirements: identification of electrons which requires a pion suppression factor of the order of 10^5, identification of hadrons with

large acceptance, determination of the primary and secondary vertices (accuracy $\sim$30 μm), high granularity of the detectors, fast detector response and read-out, very small detector dead time, high-speed trigger and data acquisition, radiation hard detectors and electronics, tolerance towards delta-electrons.

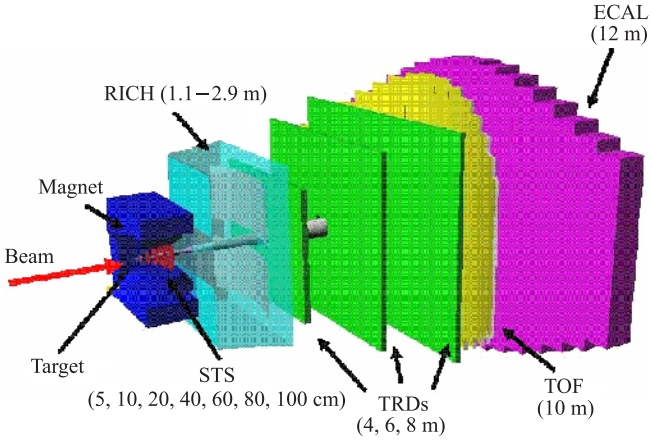

Fig. 1. CBM general layout

Figure 1 depicts the present layout of the CBM experimental set-up. Inside the dipole magnet gap there are a target and a 7-planes Silicon Tracking System (STS) consisting of pixel and strip detectors. The Ring Imaging Cherenkov detector (RICH) has to detect electrons. The Transition Radiation Detector (TRD) arrays measure electrons with momentum above 1 GeV. The Time-of-Flight (TOF) detector consists of Resistive Plate Chambers (RPC). The Electromagnetic Calorimeter (ECAL) measures electrons, photons and muons. The CBM set-up is optimized for heavy-ion collisions in the beam energy range from about 8 up to 45A GeV. The typical central Au + Au collision in the CBM experiment will produce up to 700 tracks in the inner tracker (see Fig. 2).

Large track multiplicities together with the presence of a non-homogeneous magnetic field make the reconstruction of events extremely complicated. It comprises local track finding and fitting in the STS and TRD, ring finding in RICH, cluster reconstruction in ECAL, global matching between STS, RICH, TRD, TOF and ECAL, and the reconstruction of primary and secondary vertices. Therefore, the collaboration performs the extensive analysis of different event recognition and reconstruction methods, in order to understand better the geometry of detectors and to investigate specific features of useful events [4].

The measurement of charmonium is one of the key goals of the CBM experiment. The main difficulty lies in the extremely low multiplicity expected in Au + Au 25A GeV collisions near J/ψ production threshold. For detecting J/ψ meson in its dielectron decay channel the main task is the separation of electrons and pions. One of the most effective detector for electron/pion separation is the TRD detector.

The TRD must provide electron identification and tracking of all charged particles. It has to provide, in conjuction with the RICH and the electromagnetic calorimeter, a sufficient electron identification capability for the measurements of charmonium and low-mass vector

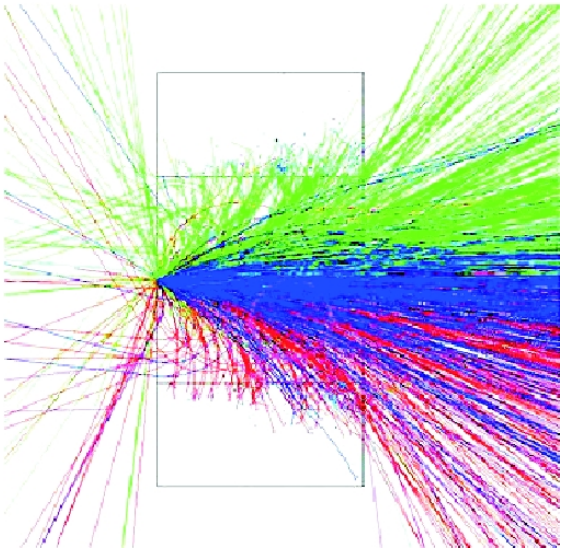

Fig. 2. Visualization of a typical CMB event

mesons. The required pion suppression is a factor of about 100 and the required position resolution is of the order of 200–300 μm. In order to fulfil these tasks, in the context of the high rates and high particles multiplicities in CBM, a careful optimization of the detector is required.

In the technical proposal of the CBM experiment, preliminary results on the estimation of the electron identification and pions suppression applying a maximum likelihood ratio test were presented (see details in [4]). A standalone Monte Carlo C++ based simulation code was developed to perfom the simulations. The following processes were considered in the simulations: i) energy losses of electrons and pions in the gas detector due to the procedure described in [2]; ii) for electrons, production and absorption of the transition radiation (TR) in the radiator, absorption of TR in the mylar foil and absorption of TR in the active gas volume. The results of these simulations demonstrated that the TRD with 9 to 12 layers can fulfil the required electron/pion indentification in CBM.

It is useful to note that the application of a maximum likelihood ratio test requires a very accurate determination of distribution functions of energy losses by pions and electrons (see details on page 88 in [4]), which is not so simple to fulfil in practice.

Recently, the use of artificial neural networks in multi-dimensional data analysis has become widespread [5–8]. One of such problems consists in classifying the individual events represented by empirical samples of finite volumes pertaining to one of the different distributions composing the distribution to be analyzed. A layered feed-forward network — multilayer perceptron (MLP) — is a convenient tool for constructing multivariate classifiers, although its learning speed and power of recognition critically depend on the choice of input data.

In [1] we investigated a possibility to apply the MLP for identification of electrons and pions using the measurements of ionization energy losses and transition radiation in the TRD detector. We demonstrated that applying the ANN one can reach a reliable level of pions suppression and electrons identification [1].

In our studies [9–11] we showed that such a type of problems could be effectively solved with the help of nonparametric ω_n^k goodness-of-fit criteria. In this work we present the results of solving this problem by applying the ω_n^k test and its comparision with the MLP method.

1. SELECTION ALGORITHMS BASED ON STATISTICAL GOODNESS-OF-FIT CRITERIA

The testing of the experimental data correspondence to some theoretical hypotheses is one of the most important part of the data analysis. In order to present the main concept of the hypothesis testing, let us recall some definitions. The hypothesis which can be formulated with no additional assumptions is called a simple hypothesis. The hypothesis which consists of a few simple hypotheses is called a complex hypothesis. In order to present the hypothesis testing, it is enough to consider only the simple hypothesis [12].

Let us test the hypothesis H_0 (called the null-hypothesis) against the alternative hypothesis H_1 using a set of experimental data. Let X be some function of observables, calling the *test statistics*, and W be the space of all possible values of X. We divide W into *critical* w and *admissible* $(W - w)$ regions so that if the values of function X hit in the region w, then the null-hypothesis is not correct. Thus, the choice of the testing criterion H_0 is reduced to the choice of the testing statistics X and the critical region w.

The size of the admissible region is usually chosen in order to get the prescribed *significance level* α, determined as probability of X to hit into w, when the hypothesis H_0 is valid:

$$P(X \in w|H_0) = \alpha. \tag{1}$$

Therefore, α is the probability that H_0 is rejected while it is correct.

The efficiency of a testing criterion depends on its ability to separate the given hypothesis H_0 from the alternative hypothesis H_1. The measure of usefulness of a criterion is given by a *criterion power*. The criterion power is determined as the probability $1 - \beta$ of X to hit into the critical region when H_1 is correct:

$$P(X \in w|H_1) = 1 - \beta. \tag{2}$$

In other words, β is the probability of X to hit into the admissible region if the alternative hypothesis is correct:

$$P(X \in W - w|H_1) = \beta. \tag{3}$$

There are two different kinds of errors in the hypothesis testing:

a) error of the first kind (or *loss*): rejection of the null-hypothesis, when it is correct. The probability of such an error is equal to α;

b) error of the second kind (or *admixture*): acceptance of the null-hypothesis, when it is not correct. The probability of such an error is equal to β.

The test criteria that check the correspondence of pre-assigned hypothesis (the null-hypothesis H_0) against all possible alternative hypotheses are called the *goodness-of-fit* criteria [12]. Such criteria test experimental data against the density function which corresponds to the hypothesis H_0, in accordance with which the testing data must be distributed.

Motivated by a practical point of view, here we will consider only the criteria which are independent of the form of the testing distribution. The most efficient criteria are based on

comparison of the distribution function $F(x)$ corresponding to the null-hypothesis H_0 with the empirical distribution function $S_n(x)$ [12]:

$$S_n(x) = \begin{cases} 0, & \text{if} \quad x < x_1; \\ i/n, & \text{if} \quad x_i \leqslant x \leqslant x_{i+1}, \quad i = 1, \ldots, n-1. \\ 1, & \text{if} \quad x_n \leqslant x, \end{cases} \tag{4}$$

Here $x_1 \leqslant x_2 \leqslant \ldots \leqslant x_n$ is the ordered sample (*variational series*) of the size n constructed on the basis of observations of the variable x.

The testing statistics is a measure of «distance» between the theoretical $F(x)$ and empirical $S_n(x)$ distribution functions. The well-known goodness-of-fit test, the Smirnov–Cramer–Mises criterion (also known as ω^2-criterion [13, 14]), is based on the statistics

$$\omega_n^2 = \int\limits_{-\infty}^{\infty} [S_n(x) - F(x)]^2 f(x) dx, \tag{5}$$

where $f(x)$ is the density function corresponding to the null-hypothesis H_0. Such sort statistics are also known as *non-parametric* statistics.

In paper [9] a new class of non-parametric statistics

$$\omega_n^k = n^{k/2} \int\limits_{-\infty}^{\infty} [S_n(x) - F(x)]^k f(x) dx, \tag{6}$$

which generalize the statistics (5), has been suggested and investigated. The values of statistics (6) can be calculated with a simple algebraic formula

$$\omega_n^k = -\frac{n^{k/2}}{k+1} \sum_{i=1}^{n} \left\{ \left[\frac{i-1}{n} - F(x_i) \right]^{k+1} - \left[\frac{i}{n} - F(x_i) \right]^{k+1} \right\}. \tag{7}$$

These statistics have a higher power for the bigger parameter k, and are more convenient for analysis when the alternative hypothesis has a two-sided form.

As it has been mentioned above, the goodness-of-fit criteria constructed on the basis of statistics (7) are usually applied for testing the correspondence of each sample (event) to the distribution known *a priori*.

On the basis of the ω_n^k criteria, a very efficient procedure has been developed and applied for identification of rare multi-dimensional events [10, 11, 15]. This algorithm includes the following steps:

1. The sample to be analyzed is transformed («normalized») so that the contribution of a dominant distribution (in most cases this distribution concerns the background process) is described by the distribution function $F_b(x)$.

2. Each sample, composed of values pertaining to the transformed distribution, is tested with the ω_n^k goodness-of-fit criterion for correspondence to the $F_b(x)$ hypothesis. In this process the abnormal events, which do not comply with the null-hypothesis, correspond to large absolute values of the ω_n^k-statistic, resulting in their clustering in the critical region.

3. The events that happen to be in the critical region are further subjected to the second test in accordance with items 1) and 2). The only difference in the second test compared to the

first one is that now the abnormal (signal) events are collected in the admissible region (using the corresponding distribution function $F_s(x)$). This results in the additional suppression of *background* events.

The statistical goodness-of-fit criterion discussed above is quite efficient in the identification of rare events, because it is powerful and statistically justified. However, to apply this criterion, one has to construct a distribution function corresponding to the analyzed process and to determine the sample size and the preparation procedure for the analyzed sample.

2. THE e/π IDENTIFICATION USING THE ω_n^k TEST

Signal events were calculated as a mixture of J/ψ electrons generated by PLUTO [16] and minimum bias Au + Au 25A GeV UrQMD [17] events (one J/ψ per UrQMD event). The J/ψ multiplicity ($1.92 \cdot 10^{-5}$) was extracted from Table 12.2 «Particle multiplicities calculated for central Au + Au collisions» [4] and multiplied by branching ratio 0.06 for dielectron mode. This means that approximately one J/ψ would be detected every 10^7 events. A corresponding background was calculated as Au + Au 25A GeV UrQMD central events.

Simulations of signal and background events were performed with the CBM software framework CBMROOT (based on ROOT package [18]), using GEANT3 [19] transport through standard set-up with a gold target 250 μm thickness, the beam pipe, STS, RICH and TRD. Only electrons (signal and background) and pions (background) which made hits in 6 STS stations and 12 TRD layers participated in J/ψ reconstruction. Electron transition radiation energy loss in the TRD gas was added to GEANT dE/dx. A schematic view of the TRD used for simulation is shown in Fig. 3.

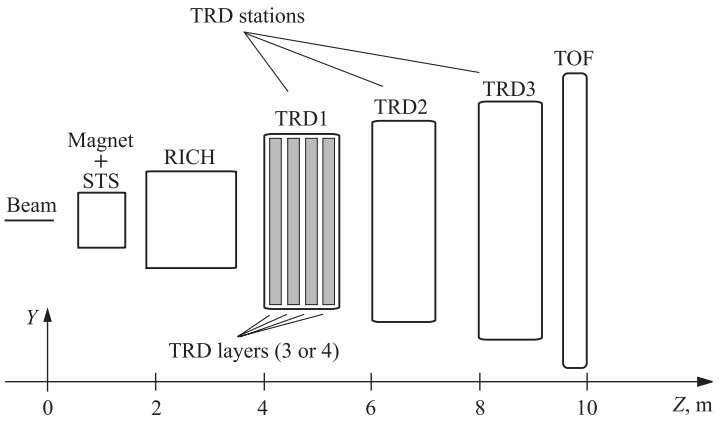

Fig. 3. Schematic view of the TRD in the CBM layout

Two types of files were formed on the basis of data generated with the help of the GEANT3 code. The first included information on ionization energy losses by pions in $n = 12$

modules of the TRD, and the second involved information on energy losses by electrons, including the transition radiation. Each file included 2500 events[1].

Figure 4 shows the distributions of energy losses (including transition radiation) by electrons (Fig. 4, *a*) and energy losses by pions (Fig. 4, *b*) in the first TRD absorber. The distributions of energy losses in other TRD absorbers have a similar character. The distributions of energy losses by pions have a Landau distribution form [20], and it is reasonable to use this distribution as a null-hypothesis for initial data transformation.

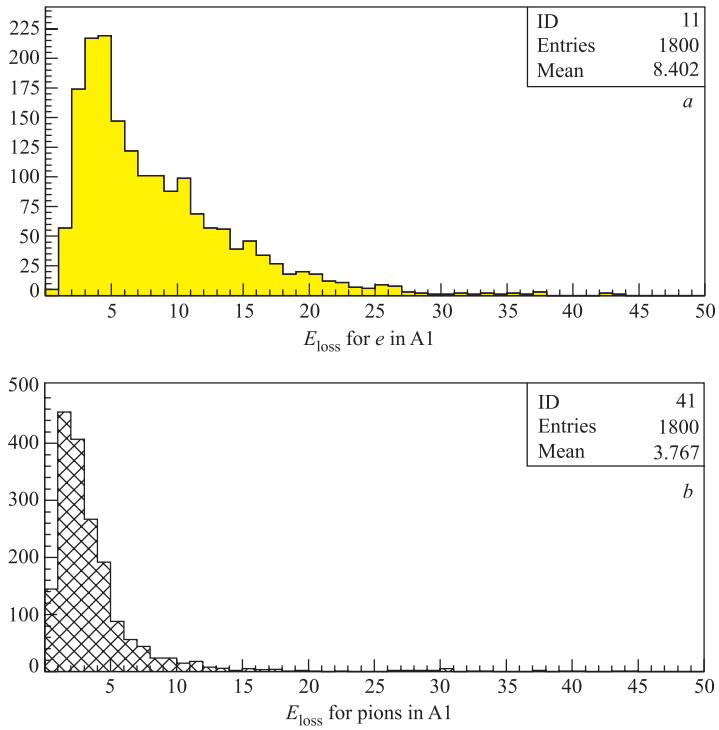

Fig. 4. Distributions of energy losses (including transition radiation) by electrons (*a*) and energy losses by pions (*b*) in the first TRD absorber

Following the algorithm described in the previous section, we transfom the initial measurements to the set of a new variable λ (see details in [11]):

$$\lambda_i = \frac{\Delta E_i - \Delta E^i_{\text{mp}}}{\xi_i} - 0.225, \qquad i = 1, 2, \ldots, n, \tag{8}$$

where ΔE_i is the value of energy loss in the ith absorber of the TRD; ΔE^i_{mp} — the value of

[1]By event we mean a sample of the volume $n = 12$ composed from energy losses of pion or electron detected by the TRD.

most probable energy loss; $\xi_i = \dfrac{1}{4.02}$ FWHM (full width on height medium) of distribution of energy losses of pions in the ith absorber [12]; n — the number of layers in the TRD.

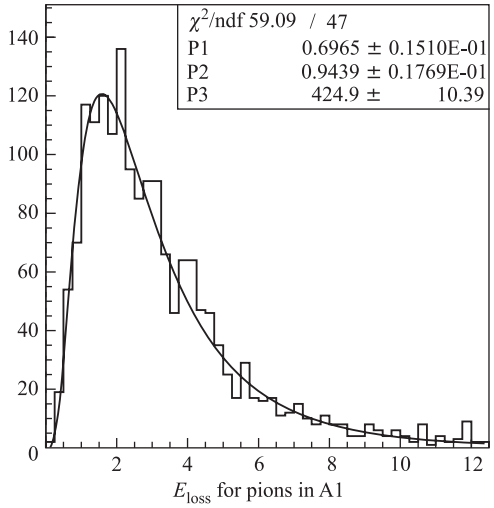

Fig. 5. Approximation of energy losses of pions in the first absorber of the TRD by the density function of the log-normal distribution (5)

In order to determine the value of most probable energy loss $\Delta E^i_{\rm mp}$ and the value FWHM of distribution of energy losses of pions in the ith absorber, the indicated distributions were approximated by the density function of a log-normal distribution (see Fig. 5)

$$f(x) = \frac{A}{\sqrt{2\pi}\sigma x} \exp\left(-\frac{1}{2\sigma^2}(\ln x - \mu)^2\right), \tag{9}$$

where σ is the dispersion; μ is the mean value, and A is a normalizing factor [12]. As one can see from Fig. 5, the distribution of energy losses by pions quite well follows the distribution (9).

The sample of obtained values $\lambda_i,\ i = 1, \ldots, n$ was ordered due to values ($\lambda_j,\ j = 1, \ldots, n$) and then used for ω_n^k calculation:

$$\omega_n^k = -\frac{n^{k/2}}{k+1} \sum_{j=1}^{n} \left\{ \left[\frac{j-1}{n} - \phi(\lambda_j)\right]^{k+1} - \left[\frac{j}{n} - \phi(\lambda_j)\right]^{k+1} \right\}. \tag{10}$$

Here the values of Landau distribution functions $\phi(\lambda)$ were calculated with the help of the DSTLAN function (from the CERNLIB library [24]).

Figure 6 presents the distributions of ω_n^k values ($k = 8$ and $n = 12$) obtained as a result of processing the generated data files for pion (*a*) and electron (*b*) events; the summary distribution is shown in (*c*).

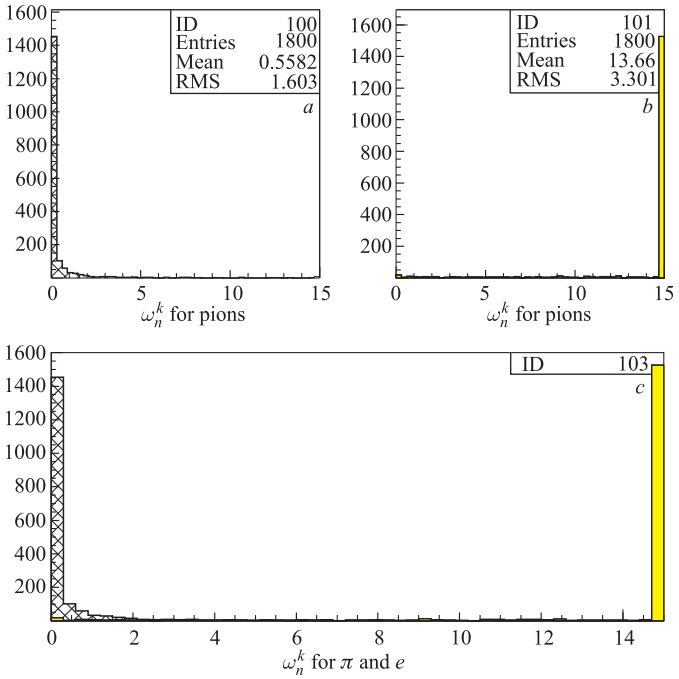

Fig. 6. Distributions of ω_n^k ($k = 8$ and $n = 12$) values obtained as a result of processing the generated data files for pion (*a*) and electron (*b*) events; the summary distribution is presented in (*c*)

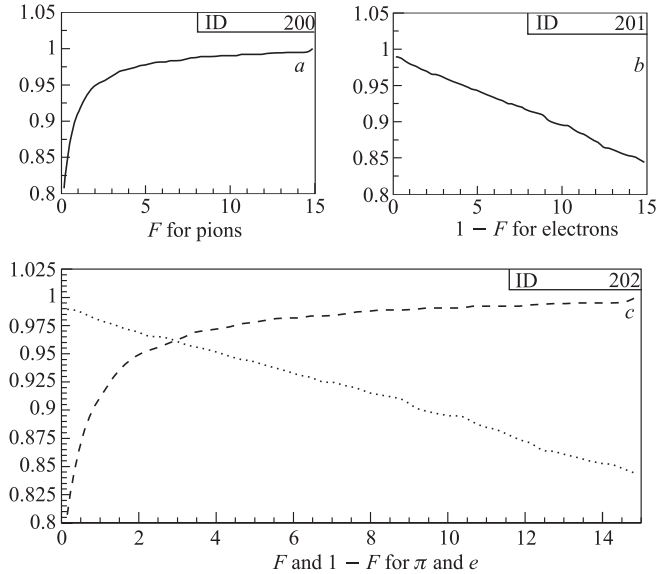

Fig. 7. The cumulative probabiliy $F(y_t) = P_r(y < y_t)$ for pion events (*a*), and the dependence $1 - F(y_t)$ for electron events (*b*); the summary dependence for pions and electrons is presented in (*c*)

Figure 7 shows the cumulative probabiliy $F(y_t) = P_r(y < y_t)$ for events corresponding to pions, and the dependence $1 - F(y_t)$ for events caused by electrons; the summary dependence for pions and electrons is presented in the Fig. 7, *c*.

3. COMPARATIVE ANALYSIS OF e/π IDENTIFICATION USING ω_n^k TEST AND ANN

In work [1] we investigated a possibility to apply a feed-forward neural network for solution of the considering problem. The three-layered perceptron from the package JETNET3 [23] has been used for particle identification. The network included $n = 12$ input neurons (according to the number of absorbers in the TRD), 35 neurons in the hidden layer and one output neuron. It was assumed that for pion events the output signal must equal -1, and for electron events — $+1$. An algorithm of the backward error propagation has been used for the error functional minimization at the stage of the ANN training [22].

In spite of the fact that the distribution of energy losses by electrons, significantly differs from the character of the distribution of energy losses by pions, when we used as input data for the MLP training the set of energy losses $\Delta E_i,\ i = 1, \ldots, n$ corresponding to the pion or electron passage through the TRD, then the training process was going on very slow. There also were large fluctuations (against the trend) of the efficiency of event identication by the network. Moreover, in spite of a large number of training epoches, one cannot reach the needed level of pions suppression.

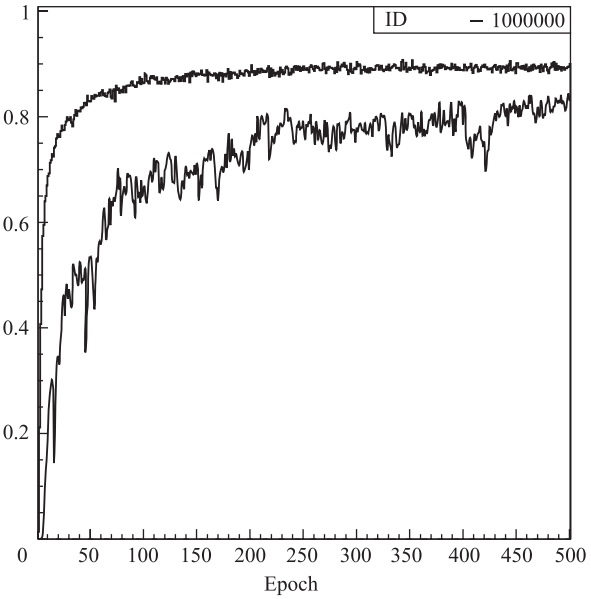

Fig. 8. The efficiency of particle identification by the MLP for original (bottom curve) and transformed (top curve) samples

In this connection, we applied to the initial data the transformation procedure described in the previous section. After this, the reliable level of pion/electron identification by the network

is reached after 10–20 training epoches in conditions of practical absence of fluctuations against the trend, and very quickly the needed level of pions suppression under the condition of a minimal loss of electrons (see Fig. 8) has been obtained.

Figure 9 presents the distributions of the MLP output signals at training (*a*) and testing (*c*) stages; *b* and *d* show the distributions of errors between the target value and the MLP output signals at the training (*a*, *b*) and testing (*c*, *d*) stages.

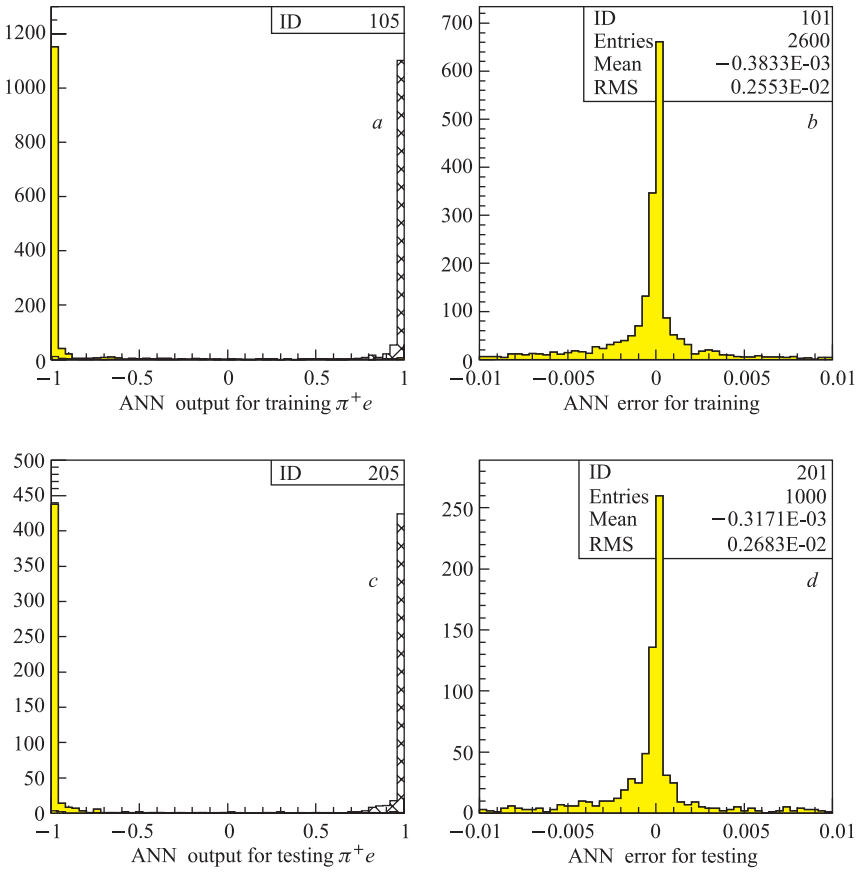

Fig. 9. Distributions of the MLP output signals at training (*a*) and testing (*c*) stages; *b*, *d* show the distributions of errors between the target value and the MLP output signals at training (*a*, *b*) and testing (*c*, *d*) stages

At the stage of network testing the event type was determined by the value of the output signal y: when it does not exceed the pre-assigned threshold y_t, the event is assumed to belong to pion, in the opposite case — to electron. Figure 10 shows the cumulative probability $F(y_t) = P_r(y < y_t)$ for events corresponding to pions and the dependence $1 - F(y_t)$ — for events caused by electrons.

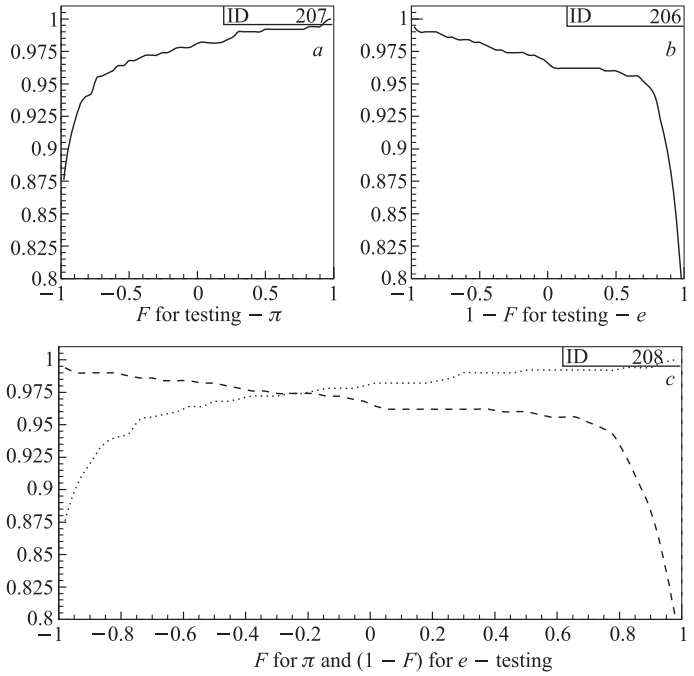

Fig. 10. The cumulative probability (for the testing stage) $F(y_t) = P_r(y < y_t)$ for events corresponding to pions (*a*) and the dependence $1 - F(y_t)$ for events caused by electrons (*b*); *c* shows the summary dependence for pions and electrons

For threshold $y_t = 0.84$ the error of the first kind α — part of electron events interpreted as pion events — was around 9.4%, and the error of the second kind β — part of pion events interpreted as electron events — was 0.6%. Thus, the suppression of pion events equals 167. In the case, when we do not apply the above-described transformation to the initial data, $\alpha = 9.1\%$, $\beta = 2.6\%$, and the suppression of pion events will consist of approximately 39.

If we choose for the ω_n^k test the threshold value $y_t = 11.0$, then the error of the first kind $\alpha = 11\%$, $\beta = 0.78\%$, and the suppression of pion events will be around 128. The obtained level of pions suppression could be increased, if we apply an additional testing of events selected in the critical region: see item 3) of the procedure described in Sec. 1.

Thus, the both approaches give comparable results of pions suppression under the condition of minimal loss of electron events.

4. THE ω_n^k-TEST IMPLEMENTATION TO e/π SEPARATION BY TRD

From Monte-Carlo (MC) simulation we exactly know which particle we deal with, and one can choose for combinatorial background only «real» electrons. After reconstruction of a charged particle trajectory in the STS detector only momentum and charge of a track are

known. For particle identification RICH and TRD detectors should be used. RICH could suppress pions with momentum below 9 GeV with a rejection factor 100. Unfortunately, J/ψ electrons have momentum 5–20 GeV/c. For a good signal-to-background ratio, the electron identification purity is a crucial factor.

The reconstructed track participates in a combinatorial background if it satisfies the following criteria:

a) track vertex is inside the target;

b) transverse momentum p_t is more than 1.2 GeV/c;

c) RICH identifies track as electron: the ring produced by this track has radius from 5.9 to 7 cm;

d) TRD identifies track as an electron: full energy loss in all TRD layers is more than 70 keV (see Fig. 11).

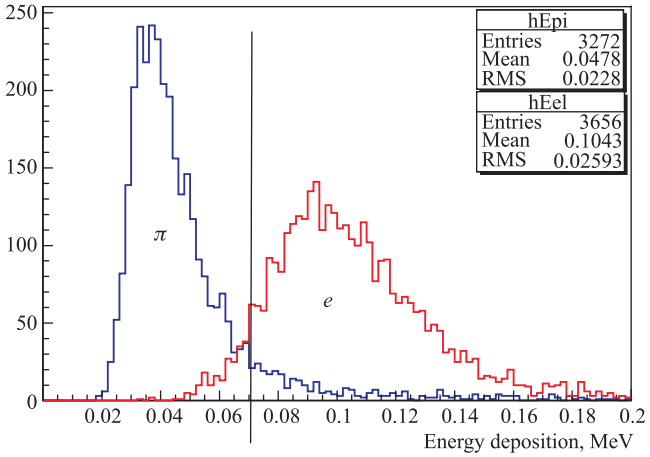

Fig. 11. Energy losses in all TRD layers for pions and electrons

In order to increase the number of background events, a super-event technique has been used. All electrons survived after «abcd» cuts were mixed together, and each e^+ was combined with each e^-. This trick allowed one to simulate the background from $10^5 \times 10^5 = 10^{10}$ events.

After these cuts 5% of the pions survived were identified as electrons. The signal-to-background ratio is approximately 1/100. Figure 12 shows dielectron invariant mass spectra for signal (bottom peak) and background (top histogram) after applying the «abcd» cuts.

Figure 13 shows the distribution of ω^8_{12} values for pions that had survived after «abcd» cuts. It is clear that additional cut $\omega^8_{12} > 11$ could eliminate most of the survived pions. Figure 14 presents the distribution of ω^8_{12} values for electrons selected after applying the «abcd» cuts. It shows that due to the $\omega^8_{12} > 11$ cut we lose approximately 10% of electrons.

Figure 15 shows the invariant mass spectra for reconstructed background particles, identified as electrons by RICH and TRD, before (bottom histogram) and after (top histogram) applying the cut $\omega^8_{12} > 11$. An intermediate distribution (MC) is an invariant mass spectrum of particles identified as electrons in simulation («real» physical electron background from

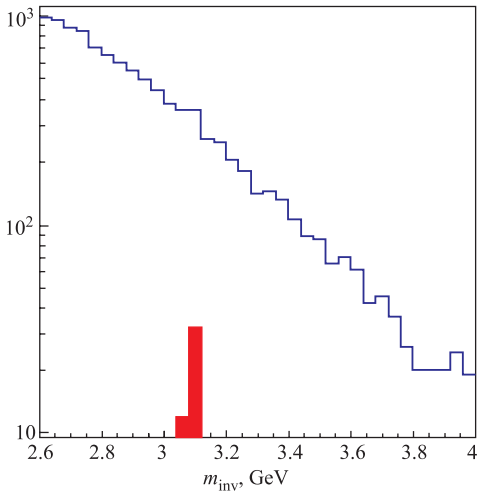

Fig. 12. Dielectron invariant mass spectra for background (top histogram) and J/ψ (bottom peak) after application cuts «abcd»

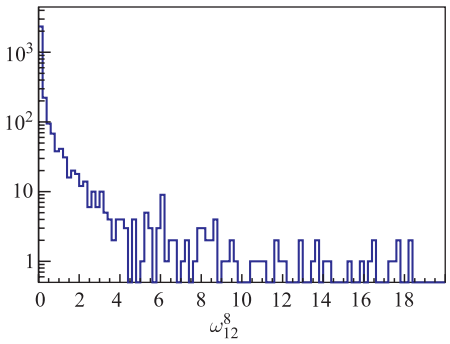

Fig. 13. Distribution of ω_{12}^8 values for pions that survived after application of «abcd» cuts

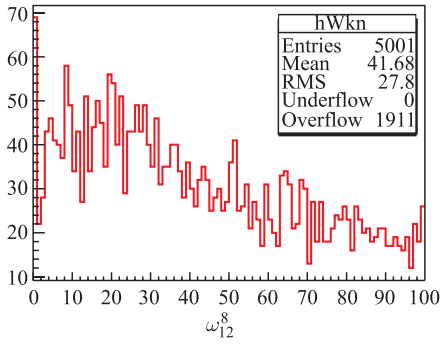

Fig. 14. Distribution of ω_{12}^8 values for electrons selected after application of «abcd» cuts

gamma-conversion, π^0 Dalitz decay and so on). One could see that almost all «real» pions (and part of «real» electrons) were rejected after application of the $\omega_{12}^8 > 11$ cut.

Figure 16 shows the invariant mass spectrum for particles identified as electrons by RICH and TRD for J/ψ and corresponding amount of central background events after applying the $\omega_{12}^8 > 11$ cut in addition to the «abcd» cuts. A comparison of the signal-to-background ratio on this plot and Fig. 12 show that the $\omega_{12}^8 > 11$ cut improves the signal/background ratio up to $\sim$100 times.

Figures 17 and 18 show a phase space coverage (p_t vs rapidity distribution) of the identified J/ψ after applying the «abcd» cuts (Fig. 17) and for the «abcd» cuts together with the $\omega_{12}^8 > 11$ cut (Fig. 18). Clearly, the $\omega_{12}^8 > 11$ cut does not change the phase space of J/ψ events.

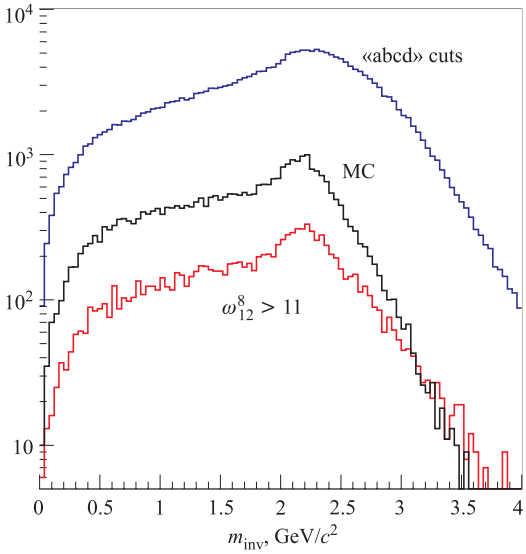

Fig. 15. Background invariant mass spectra for particles identified as electrons: top histogram — the «abcd» cuts are applied; medium histogram — MC («real») background; bottom histogram — in addition to the «abcd» cuts the $\omega^8_{12} > 11$ is applied

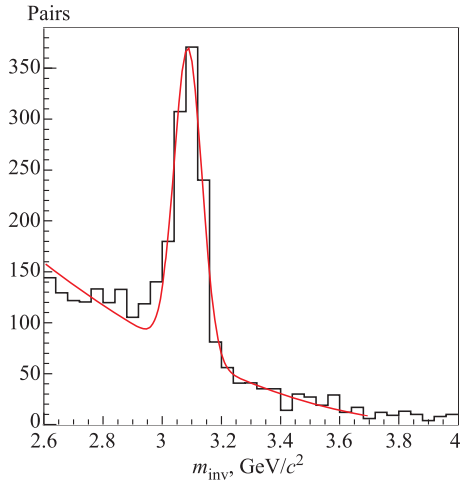

Fig. 16. Invariant mass spectrum for particles identified as electrons by RICH and TRD for J/ψ and corresponding amount of central background events after applying «abcd» and $\omega^8_{12} > 11$ cuts

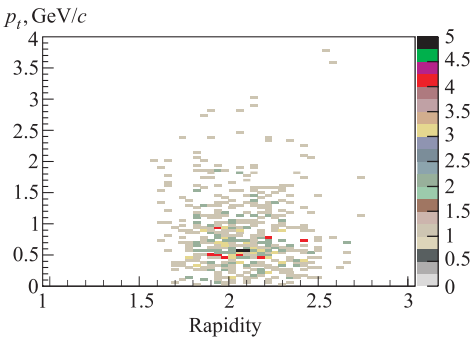

Fig. 17. p_t vs rapidity distribution for J/ψ with «abcd» cuts

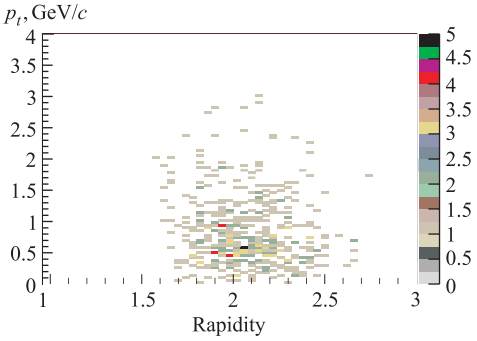

Fig. 18. p_t vs rapidity distribution for J/ψ with «abcd» and $\omega^8_{12} > 11$ cuts

In the Table we present summary results of J/ψ efficiency together with a corresponding signal-to-background (S/B) ratio for different cuts.

The J/ψ efficiency and signal-to-background ratio for different cuts

Type of cuts	No cuts	$p_t > 1.2$ GeV/c	«abcd»	«abcd»+$\omega^8_{12} > 11$
J/ψ eff	0.37	0.24	0.19	0.156
S/B ratio	0.0000	1.24	0.01	1.7

CONCLUSION

We present the electron/pion identification using energy losses in 12 layers of the CBM TRD detector applying the ω_n^k test. We show that under the loss of approximately 10–11% of electron events we may achieve the suppression of pion events up to the acceptable level (taking into account the requirements of the physical problem) equal to 0.78%, which corresponds to the suppression of pion events up to 130 times. The comparision of this approach with the algorithm based on ANN has shown that both methods provide comparable results. At the same time, it must be noted that:

1. The algorithm on the ANN basis reached the result close to the result on the ω_n^k test basis only after the application to the initial sample $\{\Delta E_i, i = 1, \ldots, n\}$ the transformation, which is typical of nonparametric goodness-of-fit criteria.

2. To apply the ANN method, one needs distributions of both competing processes (distributions of energy losses of pions and electrons), while the usage of the ω_n^k test requires only the parameters of dominate distribution (in our case, the distribution of pion energy losses).

3. The ω_n^k-criteria usage is substantiated quantitatively, while the results yielded by the ANN are only qualitative.

We demonstrate that the application of the ω_n^k criterion to the J/ψ reconstruction procedure gives a very good suppression of a pion background and significantly improves a signal-to-background ratio.

REFERENCES

1. *Akishina E. P. et al.* Electron/Pion Identification in the CBM TRD Applying a Multilayer Perceptron. JINR Commun. E10-2007-17. Dubna, 2007.
2. *Andronic A. et al.* // Nucl. Instr. Meth. A. 2004. V. 519. P. 508.
3. Letter of Intent for the Compressed Baryonic Matter Experiment. http://www.gsi.de/documents/DOC-2004-Jan-116-2.pdf
4. Compressed Baryonic Matter Experiment. Technical Status Report, GSI. Darmstadt, 2005. http://www.gsi.de/onTEAM/dokumente/public/DOC-2005-Feb-447 e.html
5. *Nauman Th. et al.* Multidimensional Data Analysis // Formulae and Methods in Experimental Data Evaluation. Geneva: Eur. Phys. Soc., 1983. V. 3.
6. *Denby B.* Tutorial on Neural Networks Applications in High Energy Physics: 1982 Perspective // Proc. of the Second Intern. Workshop on Software Engineering, Artificial Intelligence and Expert System in High Energy Physics, L'Agelaude France-Telecom La Londe-les-Maures, 1992. P. 287.
7. *Kisel I. V., Neskoromnyi V. N., Ososkov G. A.* Application of Neural Networks in Experimental Physics // Part. Nucl. 1993. V. 24. P. 1551.
8. *Ivanov V. V. et al.* JINR Preprint P10-94-300. Dubna, 1994.
9. *Ivanov V. V., Zrelov P. V.* Nonparametric Integral Statistics $\omega_n^k = n^{k/2} \int_{-\infty}^{\infty} [S_n(x) - F(x)]^k dF(x)$: Main Properties and Applications // Intern. J. Comput. & Math. with Appl. 1997. V. 34, No. 7/8. P. 703–726; JINR Commun. P10-92-461. Dubna, 1992 (in Russian).

10. *Zrelov P. V., Ivanov V. V.* The Small Probability Events Separation Method Based on the Smirnov–Gramer–Mises Goodness-of-Fit Criterion: Algorithms and Programs for Solution of Some Problems in Physics. V. 6. Preprint KFKI-1989-62/M. Budapest, 1989. P. 127–142.

11. *Zrelov P. V., Ivanov V. V.* The Relativistic Charged Particles Identification Method Based on the Goodness-of-Fit ω_n^3-Criterion // Nucl. Instr. Meth. A. 1991. V. 310. P. 623–630.

12. *Eadie W. T. et al.* Statistical Methods in Experimental Physics. Amsterdam; London: North-Holland Pub. Comp., 1971.

13. *Cramer H.* Mathematical Methods of Statistics. Univ. of Stockholm, 1946.

14. *Martinov G. V.* Omega-Squared Criteria. M.: Nauka, 1978 (in Russian).

15. *Zrelov P. V.* Simulation of Experiment on the Investigation of the Processes of the Subthreshold K^+ Production. JINR Preprint P10-92-369. Dubna, 1992; Math. Modeling. 1993. V. 4, No. 11. P. 56–74 (in Russian).

16. http://www-hades.gsi.de/computing/pluto/html/PlutoIndex.html

17. *Bleicher M. et al.* Relativistic Hadron–Hadron Collisions in the Ultra-Relativistic Quantum Molecular Dynamics Model // J. Phys. G. 1999. V. 25. P. 1859.

18. ROOT — An Object-Oriented Data Analysis Framework. User's Guide V. 5.08. 2005.

19. GEANT — Detector Description and Simulation Tool. CERN Program Library, Long Write-up, W5013. 1995.

20. *Kolbig K. S., Schorr B.* // Comp. Phys. Commun. 1984. V. 31. P. 97.

21. *Fogelman Soulie F.* Neural Networks for Patterns Recognition: Introduction and Comparison to Other Techniques // Ibid. P. 277.

22. *Rumelhart D. E., Hinton G. E., Williams R. J.* Learning Internal Representations by Error Propagation // Parallel Distributed Processing: Explorations in the Microstructure of Cognition. V. 1. Foundations. MIT Press, 1986.

23. *Peterson C., Rögnvaldsson Th., Lönnblad L.* JETNET 3.0 — A Versatile Artificial Neural Network Package // Comp. Phys. Commun. 1994. V. 81. P. 185.

24. *Koelberg K. S.* CERN Computer Centre Program Library, G110.

Received on January 30, 2007.